

Experimental Study of Fluidized Bed Abrasive Jet Machining (FB-AJM) of Quartz Material with Hot Silicon Carbide (SiC) Abrasives

B. K. Nanda* and D. Dhupal

School of Mechanical Engineering, KIIT University, Bhubaneswar, Odisha-751024
Department of Production Engineering, VSSUT, Burla, Sambalpur, Odisha - 768018

Abstract

The present research work focuses on the innovative approach of using hot Silicon Carbide (SiC) abrasives for machining of Quartz materials at different temperatures. Hot abrasive Fluidized Bed Abrasive Jet Machining (FB-AJM) is a unique concept of performing the machining operations on very hard and brittle materials like quartz, glass, ceramics, and other engineering materials. The fluidized bed mixing chamber along with the pressurized powder feed system is indigenously fabricated and modified with an abrasive heating chamber set-up to study the effects of the machining parameters, namely, Pressure (P), standoff distance (S), Grain size (G), and temperature (T) on the responses like material removal rate (MRR), Surface Roughness (R_a), and Over-cut (Oc). Experiments are conducted at different parameter settings according to the Box Behnken Design of Response Surface Methodology (RSM) to study the effect of input parameters on the responses by developing regression models and desirability functions. Finally, the multi-response optimization of the input parameters for the different responses is performed with particle swarm optimization (PSO) to get the optimal setting of P, S, G, and T. Then a single experiment is performed at the predicted optimal condition to validate the model.

Keywords: FB-AJB, Quartz, RSM, Desirability, PSO

1. INTRODUCTION

Abrasive Jet Machining (AJM) is an efficacious and economic process to perform machining, drilling, surface contouring, etching, deburring, and polishing operations on hard, brittle and heat sensitive materials like ceramics, quartz, glass, semiconductor materials, super alloys, mica, refractory materials and etc. The fine abrasive particles repeatedly impinge on the target material with very high velocity so that the high amount of kinetic energy is converted into impact energy to cause initiation and propagation of lateral cracks for solid-solid erosion. Then high velocity carrier gas removes the dislodged microscopic particles from the machined surface. The accuracy and efficiency of AJM process are largely affected by the carrier gas pressure, nozzle tip distance, jet speed, grain size, grain hardness, nozzle geometry, nozzle material, incident impingement angle, and hardness of the work material. The effective utilization of the selected process parameters and their combinations make the optimization of the machining parameters for their economic and effective utilization so that large number of tedious, costly, and time consuming experiments can be reduced.

Most of the literature review of AJM explains about the influence of the process parameters that affect the overall machining characteristics like material removal rate, surface finish, over cut, flaring diameter, taper angle, and etc. some numerical analysis, experimental analysis with suitable design of experiment (DOE) followed by different techniques of optimization. Jafar et al. [1] developed the numerical model to simulate the brittle erosion of borosilicate glass in AJM process for creating unmasked channel which was a function of particle size, velocity, dose, impact angle, and properties of target material to obtain that chip removal was due to lateral cracking and profile smoothing was the contribution of edge chipping. The surface evolution models for the abrasive jet micro-machining (AJM) of metallic substrates with Al_2O_3

abrasive was applied by Ally et al. [2] to find the peak erosion rate with jet inclination angle within 20° to 35° , and predicted the cross-sectional profiles of both unmasked and masked channels which were in good agreement with the measured profiles. The predictive mathematical models for the erosion rate during machining of glasses by micro abrasive air jets was also performed using Taguchi orthogonal array to determine the constants in the models, and the predictive model was assessed and verified by an experiment [3]. The effect of particle size, velocity, and angle of attack on the roughness and erosion rate of unmasked channels machined in borosilicate glass with alumina particles in AJM was experimentally presented by Jafar et al. [4] to quantify the damage from a single impact for improving the analytical model of roughness and erosion rate. Wakuda et al. [5] compared the material erosion models of lateral and radial cracks with the earlier theories to verify the potential of AJM process as a practical micro-machining technology for ceramic materials by applying the shot blasting phenomenon of micromachining. Zhang et al. [6] applied Taguchi orthogonal array and multi-variable linear regression to micro abrasive intermittent jet machining (MAIJM) process in which no abrasive was injected into gas stream for a period of time and the continuous flow of gas without abrasives blew away any abrasive that accumulated in the hole. Balasubramaniam et al. [7,8] presented the burr model for 90° cross-drilled holes and obtained the shape of the surface generated by conducting deburring of cross-drilled holes with abrasive jet and identified the most significant parameter that affected the process. The applicable computer simulation was developed by Shafiei et al. [9] to predict the time evolution of the eroded profiles of air abrasive jet machined surfaces as a function of process parameters and studied the effects of collisions between the incoming and rebounding particles by tracking individual particles, performing inter-particle and particle-to-surface collision detection by implementing collision kinematics. Implementation of SU-8 mask for cutting micro-channels for micro-fluidic flow and fabrication of the passive micro-mixer with 3D feature was successfully performed by

* Email: basantananda_2005@yahoo.co.in

Saragih et al. [10,11] by using micro-AJM process. J.H. Ke et al. [12] developed a novel composite-abrasive made of a thermoplastic polymer with polystyrene as the base material for achieving improved surface quality of hard, and brittle materials during abrasive jet micro-machining process to prevent direct impact on the workpiece, resulting in smaller, fewer, and shallower cracks so as to increase the surface roughness. Finished surface was generated inside the cylindrical work-piece with elastic-abrasives by conducting experiments according to RSM and the effect of pressure, abrasive size and stroke velocity on surface finish were properly investigated [13]. B. C. Routara et al. [14] applied Taguchi based gray relational analysis to perform the machining of glass work pieces in AJM for determining the optimal combinations of the input parameters for the multi-responses, like MRR and surface roughness. Experiments on abrasive water jet turning for machining of alumina ceramics was performed by Liu et al. [15] using response surface methodology (RSM) design and predicted the response values at the optimal combination of the parameter settings. Jagadish et al. [16] performed experiments on abrasive water jet machining (AWJM) on green composites with response surface methodology (RSM) and optimized the process parameters. The experimentation and optimization of process parameters of abrasive water jet (AWJ) cutting process with multi-response characteristics based on "Multi Criteria Decision Making Methodology (MCDM)" using the "Technique for Order Preference by Similarity Ideal Solution (TOPSIS)" approach was successfully performed by N. Yuvaraj and M. P. Kumar [17].

The concept of fluidized bed abrasive jet machining (FB-AJM) system is to make an upward flow of high speed air from the bottom of the reservoir through the powder bed to produce a uniform air-abrasive mixture with well-regulated mass flow rate. It creates a cloud of suspended particles near the nozzle inlet, producing a uniform air-abrasive mixture with well-regulated mass flow rate. Barletta et al. [18-21] developed long tubular components made from high resistance stainless steel and high strength ductile aluminum alloy (AA 6082 T6) for achieving more regular and smoother surface finishing with the hybrid technology of fluidized bed assisted abrasive jet machining (FB-AJM) to finish the internal part of narrow and good circumferential uniformity and accuracy. The unwanted embedded abrasive particles in AJM hamper the material removal as well as a surface finish. B. K Nanda et al. [22] performed experiments on fluidized bed abrasive jet machining (FB-AJM) of alumina ceramic (K-99) using SiC abrasives to analyze the influence of process parameters on the different responses and applied the multi-objective desirability based particle swarm optimization (PSO) for predicting the optimal values, and finally these values were experimentally confirmed. N. Jagannatha et al. [23,24] used hot air as carrier media in AJM to carry out experiment on glass etching and grooving by using abrasive, hot air jet machining (AHAJM) and studied the effect of air temperature on material removal rate and surface roughness applied to the process of glass etching and grooving. This paper is focused on hot abrasive fluidized bed abrasive jet machining (FB-AJM) of hard, brittle and heat sensitive quartz materials using hot SiC abrasive at different temperatures with the FB-AJM set up based on pressurized powder feed and fluidized mixing chamber. The influence of four machining parameters viz. pressure (P), stand-off distance (S), Temperature (T), and abrasive size (G) on the responses like material removal rate (MRR), surface roughness (Ra), and taper angle (TA) are experimentally analyzed according to Box-

Behnken design of response surface methodology. Then regression models are developed, desirability functions are defined, and particle swarm optimization (PSO) technique is applied to get the optimal conditions of input parameters. Finally, these results are experimentally validated.

2. DETAIL OF EXPERIMENTATION

2.1 Experimental Procedure

All the experiments are conducted on the fluidized bed abrasive jet machine (FB-AJM) set up which is designed, fabricated and assembled as shown in Fig.1, where the feeder is modified so that the abrasive particles are heated to obtain the hot abrasive particles at required temperatures. Some designers proposed the mixing of hot air to the abrasive [23,24] but the use of hot abrasives is considered in this research work. A multi-stage air compressor of 5 kW power with 10 kgf/cm² of working pressure is used to supply high pressure air as the carrier medium. The compressed air is then passed through the dehumidifier or Filter-Regulator-Lubricator (FRL) unit to produce moisture free clean and dry air so that clogging of abrasives at nozzle exit can be prevented. D2 steel material (high carbon and high chromium steel) is used to fabricate the nozzle as it has high wear and abrasion resistance properties. The experiments are conducted inside an airtight machining chamber to prevent leak of the fine abrasive particles to the atmosphere, otherwise surrounding may be polluted.



Fig.1 FB-AJM with Hot Abrasive Chamber

2.2 Specification of Work Piece and Abrasive Materials

The hard quartz pieces of specimen size 20mm x 20mm x 4mm (with $\pm 1\%$ dimensional accuracy) are used as the workpiece



Fig.2 Quartz plates after machining

materials and silicon carbide (SiC) abrasives with average sizes of 270, 350 and 560 μ m are taken for experimentation. The quartz plates after machining and SEM of SiC abrasive are given in Fig.2 and Fig.3.

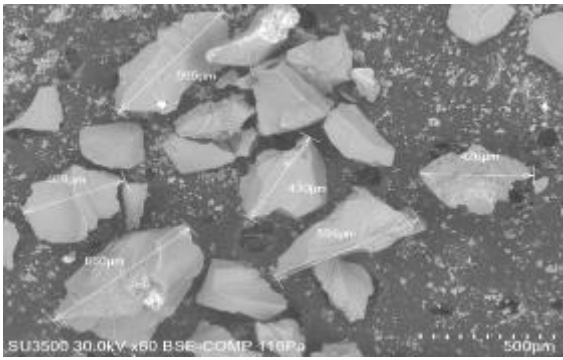


Fig.3 SEM micrograph of zircon sand abrasives

2.3 Input process parameters

The proper selection and combination of input process parameters with their levels are important to achieve the best output result. Here, pressure (P), standoff distance (S), grain size (G), and temperature (T) are taken as input parameters with their three different levels as shown in Table 1 to measure material removal rate (MRR), surface roughness (R_a), and over cut (Oc) as responses.

Table 1: Levels of input parameters

SI No	Parameter	Levels		
		Low	Mid	High
1	Pressure(Kgf/cm ²)	4	5	6
2	Temperature(°C)	40	50	60
3	Grain Size (µm)	270	350	560
4	Stand-off Distance(mm)	3	4	5

2.2.1. Measurement of Material removal rate (MRR)

Material removal rate (w) is calculated on mass (g/s) basis as, $w = \frac{(W_1 - W_2)}{\Delta t}$ where, W_1 and W_2 (gm) are the weights of the specimen before and after machining with a time span of Δt .

2.2.2 Measurement of surface roughness (R_a)

MITUTOYO 400 with least count of 0.001µm., sampling length of 0.75mm and evaluation length of 3mm is used to measure the surface roughness of the secondary etched surfaces thrice at different positions of each work piece and their average are taken as the final reading.

2.2.3 Measurement of taper angle (TA)

The drilled-hole in AJM resembles a truncated cone in which the tapered angles are generated on the surface and it is measured by measured by CMM, 876, Zeiss MC850 with stylus and a probe attachment.

3. DESIGN OF EXPERIMENT

Design of experiment (DOE) explains about the conduct of the experiment and analysis of data. Here, experiments are conducted according to Box-Behnken design (BBD) of response surface methodology (RSM) with 4 input parameters like pressure (P), stand-off distance (S), grain size (G), and each with 3 (Low, Mid and High) levels to measure MRR (W), surface roughness (R_a), and taper angle (TA). All the surface plots and statistical calculations are made with Design Expert software.

4. EXPERIMENTAL RESULTS AND DISCUSSIONS

The results obtained for the specimen (Table 2) are put in Design Expert software to find the most significant variable, p-values, Lack of Fit Values, R^2 and Adj- R^2 - values of the response models from the Analysis of Variance (ANOVA) as shown in Table 3.

Table 2: Box Behnken design based Experimental Data

Sl.No.	P	S	G	T	MRR	R_a	TA
1	4	3	350	50	0.0131696	5.7061	35.6754
2	6	3	350	50	0.0099719	9.6098	33.6244
3	4	5	350	50	0.0091630	7.4948	32.8926
4	6	5	350	50	0.0105383	5.4315	36.0140
5	5	4	270	40	0.0129294	8.7264	36.8930
6	5	4	560	40	0.0120329	7.3525	36.6537
7	5	4	270	60	0.0112890	6.4018	37.1689
8	5	4	560	60	0.0129102	5.7511	36.1610
9	4	4	350	40	0.0090171	7.4945	35.7944
10	6	4	350	40	0.0116497	6.6758	36.9010
11	4	4	350	60	0.0106720	6.7972	36.1875
12	6	4	350	60	0.0072339	8.8617	35.2171
13	5	3	270	50	0.0097796	9.3309	35.3636
14	5	5	270	50	0.0131328	7.4068	37.9864
15	5	3	560	50	0.0093157	7.5297	36.5247
16	5	5	560	50	0.0097949	8.1572	35.6625
17	4	4	270	50	0.0103199	6.4647	36.4900
18	6	4	270	50	0.0086579	6.7673	33.5544
19	4	4	560	50	0.0062760	12.8740	36.0249
20	6	4	560	50	0.0120559	7.2383	35.9747
21	5	3	350	40	0.0114323	10.0623	35.0493
22	5	5	350	40	0.0135890	8.7418	36.4695
23	5	3	350	60	0.0088007	8.0566	35.2800
24	5	5	350	60	0.0110872	6.0558	37.3491
25	5	4	350	50	0.0072549	5.8555	38.0094
26	5	4	350	50	0.0100515	7.2870	37.0469
27	5	4	350	50	0.0106921	3.9993	34.1011

Table 3 ANOVA

Response	p-value	Lack of Fit	R-squared	Adj R-squared
MRR	0.0407	0.8587	0.9329	0.8122
R_a	0.0479	0.9395	0.7571	0.7436
TA	0.0464	0.3980	0.7587	0.4772

It is observed that the p-values of all the three responses are less than 0.05 which implies that models are significant. Again, lack of fit value is non-significant, more value of R-Squared and the Model-F value is significant for each response which ensures satisfactory validation of the designed models. The regression analysis for each of the responses is performed by considering quadratic models as:

$$\begin{aligned}
 MRR = & 0.048 + 8.452 \times 10^{-3}P - 5.665 \times 10^{-3}S - 1.313 \times 10^{-4}G \\
 & - 9.439 \times 10^{-4}T + 3.933 \times 10^{-4}PS + 1.31 \times 10^{-5}PG \\
 & - 1.52 \times 10^{-4}PT - 3.538 \times 10^{-6}GS + 3.245 \times 10^{-6}ST \\
 & + 5.275 \times 10^{-7}GT - 6.932 \times 10^{-4}P^2 + 6.88 \times 10^{-4}S^2 \\
 & + 6.202 \times 10^{-8}G^2 + 1.422 \times 10^{-5}T^2
 \end{aligned} \quad (1)$$

$$Ra = 9.69627 + 2.15388P + 5.39963S - 0.0548 \times G - 0.3289T - 1.2418PS - 1.4214 \times 10^{-4} PG - 0.0271PT + 2.1727 \times 10^{-3} GS - 0.117ST + 1.5184 \times 10^{-4} GT + 0.1571P^2 + 0.7231S^2 + 4.7388 \times 10^{-5} G^2 + 5.7236 \times 10^{-3} T^2 \quad (2)$$

$$TA = 101.388 - 4.461P - 8.379S - 0.049G - 1.173T + 1.243PS + 2.8 \times 10^{-3} PG - 0.519PT - 4.18 \times 10^{-3} GS + 0.016ST - 1.226 \times 10^{-4} GT + 0.088P^2 + 0.406S^2 + 7.03 \times 10^{-5} G^2 + 0.014T^2 \quad (3)$$

4.1 Surface plot analysis

The variations of material removal rate (MRR) with pressure (P) and temperature (T) is given on the surface plots, shown in Fig.4. It is seen that initially MRR decreases with T and then increases, but MRR increases with increases in P. It is due to the achievement of higher kinetic energy of abrasive particles at higher temperature and pressure. Similarly, conclusions can be obtained from the other response plots of MRR. The variations of surface roughness (Ra) with pressure (P) and temperature (T) is given on the surface plots, shown in Fig.5, where Ra first decrease and then increases with increase in P and T, because of variations in the MRR. Similarly, the variation of Taper Angle (TA) with pressure (P) and temperature (T) is shown in Fig.6.

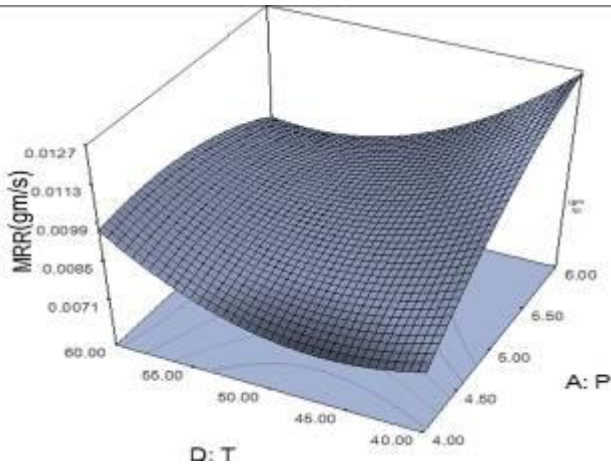


Fig.4 Variation of MRR with P and T

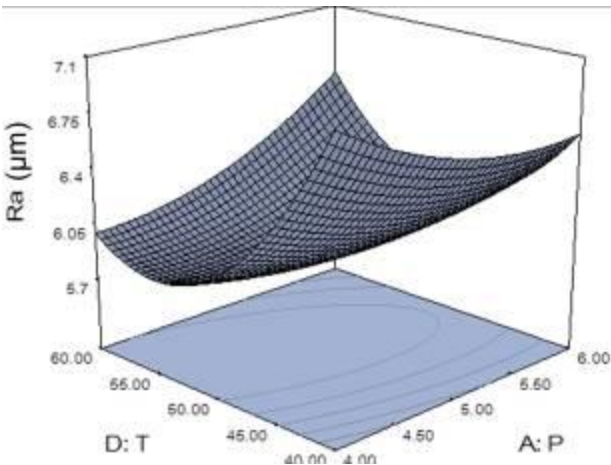


Fig.5 Variation of Ra with P and T

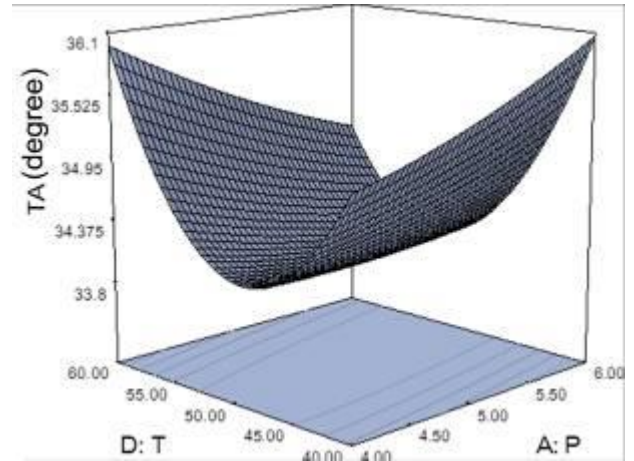


Fig.6 Variation of TA with P and T

5. DESIRABILITY BASED PARTICLE SWARM OPTIMIZATION (PSO)

5.1 Desirability Function

Desirability based multi-objective optimization was performed by Candiotti et al [25] based on the concept of Derringer and Suich, in which each and every output is converted into a global desirability function as given in equation (4) where, U_i =Upper, L_i = lower, and T_i = Target values of each output with powers “s” and “t” as the weights (w_j) set by the researcher. By combining all these individual desirability indices, the global desirability index (D) is determined as per equation (5) with n = total number of objectives, and w_j = individual weights, in a scale from 1 to 5 (1 for the least and 5 for the highest importance). The weight distribution and Desirability Function of the objectives are shown in Table 4, and desirability index D in equation.(5)

$$d_i(\hat{y}_i(x)) = \begin{cases} 0 & \text{if } \hat{y}_i(x) < L_i \\ \left(\frac{\hat{y}_i(x) - L_i}{T_i - L_i} \right)^s & \text{if } L_i \leq \hat{y}_i(x) < T_i \\ 1 & \text{if } \hat{y}_i(x) = T_i \\ \left(\frac{\hat{y}_i(x) - U_i}{T_i - U_i} \right)^t & \text{if } T_i \leq \hat{y}_i(x) \leq U_i \\ 0 & \text{if } \hat{y}_i(x) > U_i \end{cases} \quad (4)$$

and desirability index, $D = (d^{f1} \times d^{f2} \times \dots \times d^{fn})^{1/\sum w_j}$ (5)

Table 4 Assigned weights to responses

Sl. No	Output	Optimization Objective	Desirability Function (Di)	Weight (w_i)
1	MRR	Maximum	$D1 = \frac{MRR - MRR_{min}}{MRR_{max} - MRR_{min}}$	5
2	Ra	Minimum	$D2 = \frac{Ra_{max} - Ra}{Ra_{max} - Ra_{min}}$	5
3	TA	Minimum	$D3 = \frac{TA_{max} - TA}{TA_{max} - TA_{min}}$	5

The Global Desirability Function (DF_i) and Fitness Function Y

$$\text{are defined as: } D = \left(d_1^{r_1} \times d_2^{r_2} \times d_3^{r_3} \right)^{\frac{1}{\sum w_j}} \quad (6)$$

$$\text{and } Y = \frac{I}{I + DF} \quad (7)$$

5.2 Implementation of PSO

The designed particle swarm optimization (PSO) problem is presented as :

Minimize Y, subjected to $X_{min} \leq X \leq X_{max}$

where, Y is objective function , X stands for input parameter as $X = \{P, Z, G, T\}$, within the following ranges:

$4 \leq P \leq 5$, $3 \leq S \leq 5$, $270 \leq G \leq 560$, and $40 \leq T \leq 60$

An initial swarm size of 50, number of iterations 200 with constants C₁ and C₂ as 2 are put in the PSO code, and made to run in MATLAB to obtain the predicted output as given in Table 5.

Table 5 Predicted Optimal and Experimental results

Type of Model	Process Parameters				Response values		
	P	S	G	T	MRR	Ra	TA
Predicted	6	5	560	50	0.00818	6.195	36.799
Actual Experiment	6	5	560	50	0.00905	6.8212	35.490
Error %			---		10.664	10.108	3.56%

The predicted optimal values are validated experimentally to find the % of errors as shown in Table 5. Due to less % of deviation between the actual experimental value and predicted values, the PSO of the FB-AJM conditions is validated.

6. CONCLUSIONS

The following outcomes can be drawn from the above experimental analysis which is a development of the recent advances in AJM process:

- (i) Better material removal rate (MRR) is achieved at parametric combinations of high pressure, mid-value of stand-off distance, higher grain sizes, and mid values of Temperature. Surface roughness (Ra) is minimum at mid values of pressure, lower values of grain size, mid values value of stand-off distance, and mid-values of temperature. Taper angle is less at high pressure, nozzle tip distance, mid-value of grain sizes, and lower values of temperature.
- (ii) The predicted optimal combination of parameter setting are pressure of 6 kgf/cm², stand-off distance of 5 mm , grain size of 560µm and temperature of 50 for achieving the optimal output, i.e. MRR of 0.008177g/sec, surface roughness having 6.195µm, and taper angle of 36.799 degrees.
- (iii) Experiment is performed at predicted optimal conditions to validate the optimality of the model and the measured experimental responses values obtained are MRR of 0.009049 gm/sec, Ra of 6.8212µm and taper angle of 35.490 mm. The percentage of errors between the predicted models and experimental values are less and within the specified range.

ACKNOWLEDGEMENT

The authors would like to acknowledge the authority of KIIT, University and VSSUT, Burla for providing all the assistances to conduct the experiments inside their Non-Traditional Machining Laboratories.

References

- [1] Jafar R.H, Spelt J.K, and Papini M., Numerical simulation of surface roughness and erosion rate of abrasive jet micro-machined channels, *Wear*, **303** (1) (2013) 302-12.
- [2] Jafar R.H, Papini M. and Spelt J.K., Simulation of erosive smoothing in the abrasive jet micro-machining of glass. *Journal of Materials Processing Technology*, **213**(12) (2013) 2254-61
- [3] Ally S, Spelt J.K, Papini M., Prediction of machined surface evolution in the abrasive jet micro-machining of metals, *Wear*, **292** (2012) 89-99.
- [4] Fan J.M, Wang C.Y, Wang J., Modelling the erosion rate in micro abrasive air jet machining of glasses, *Wear*. **266**(9) (2009) 968-74.
- [5] Wakuda M, Yamauchi Y, and Kanzaki S., Effect of workpiece properties on machinability in abrasive jet machining of ceramic materials, *Precision engineering*; **26** (2) (2002) 193-8.
- [6] Zhang L, Kuriyagawa T, Yasutomi Y, and Zhao J., Investigation into micro abrasive intermittent jet machining, *International Journal of Machine Tools and Manufacture*. **45** (7) (2005) 873-879.
- [7] Balasubramaniam R, Krishnan J, and Ramakrishnan N. A study on the shape of the surface generated by abrasive jet machining, *Journal of Materials Processing Technology*, **121** (1) (2002) 102-6.
- [8] Balasubramaniam R, Krishnan J, and Ramakrishnan N., An empirical study on the generation of an edge radius in abrasive jet external deburring (AJED), *Journal of Materials Processing Technology*, **99**(1) (2000) 49-53
- [9] Shafiei N, Getu H, Sadeghian A, and Papini M., Computer simulation of developing abrasive jet machined profiles including particle interference, *Journal of Materials Processing Technology*; **209**(9) (2009) 4366-78.
- [10] Saragih A.S. and Ko T.J., A thick SU-8 mask for microabrasive jet machining on glass. *The International Journal of Advanced Manufacturing Technology*, **41**(7), (2009) pp.734-740.
- [11] Saragih A.S., and Ko T.J., Fabrication of passive glass micromixer with third-dimensional feature by employing SU8 mask on micro-abrasive jet machining. *The International Journal of Advanced Manufacturing Technology*, **42**(5-6) (2009), pp.474-481.
- [12] Ke J.H., Tsai, F.C., Hung, J.C., Yang T.Y., and Yan B.H., Fabrication of new composite, abrasive for jet machining and application to scrap wafer regeneration. *Proceedings of the Institution of Mechanical Engineers, Part E: Journal of Process Mechanical Engineering*, **226**(1) (2012), pp.3-11.
- [13] Sooraj V.S. and Radhakrishnan V., Fine finishing of internal surfaces using elastic abrasives, *International Journal of machine tools and manufacture*, **78**, (2014) pp.30-40.
- [14] Routara B.C., Nanda B.K., Sahoo A.K., Thatoi D.N. and Nayak B.B., Optimisation of multiple performance characteristics in abrasive jet machining using grey relational analysis, *International Journal of Manufacturing Technology and Management*, **24**(1-4), (2011), pp.4-22.
- [15] Liu D., Huang C., Wang, J., Zhu, H., Yao, P. and Liu, Z., Modeling and optimization of operating parameters for abrasive waterjet turning alumina ceramics using response surface methodology combined with Box-Behnken design. *Ceramics International*, **40**(6) (2014), pp.7899-7908.

- [16] Jagadish, Bhowmik S. and Ray A., Prediction and optimization of process parameters of green composites in AWJM process using response surface methodology, *The International Journal of Advanced Manufacturing Technology*, 87 (5-8), (2016), pp.1359-1370.
- [17] Yuvaraj N. and Pradeep K M., Multiresponse optimization of abrasive water jet cutting process parameters using TOPSIS approach. *Materials and Manufacturing Processes*, 30(7), (2015) pp.882-889.
- [18] Barletta M., A new technology in surface finishing: fluidized bed machining (FBM) of aluminium alloys, *Journal of materials processing technology*, 173(2), (2006), pp.157-165
- [19] Barletta M., Guarino S., Rubino G. and Tagliaferri V., Progress in fluidized bed assisted abrasive jet machining (FB-AJM): Internal polishing of aluminium tubes, *International Journal of Machine Tools and Manufacture*, 47(3), (2007), pp.483-495.
- [20] Barletta M., Ceccarelli D., Guarino S. and Tagliaferri V., Fluidized bed assisted abrasive jet machining (FB-AJM): precision internal finishing of Inconel 718 components, *Journal of Manufacturing Science and Engineering*, 129(6), (2007), pp.1045-1059
- [21] Barletta M., Rubino G., Guarino S., Bolelli, G., Lusvarghi L. and Gisario A., Fast regime-fluidized bed machining (FR-FBM) of atmospheric plasma spraying (aps) TiO₂ coatings. *Surface and Coatings Technology*, 203(5) (2008), pp.855-861.
- [22] Nanda B.K., Mishra A. and Dhupal D., Fluidized bed abrasive jet machining (FB-AJM) of K-99 alumina ceramic using SiC abrasives, *The International Journal of Advanced Manufacturing Technology*, 90(9-12), (2017), pp.3655-3672.
- [23] Jagannatha, N., Hiremath, S.S. and Sadashivappa, K., 2012. Analysis and parametric optimization of abrasive hot air jet machining for glass using Taguchi method and utility concept. *International Journal of Mechanical and materials engineering*, 7(1), pp.9-15.
- [24] Jagannatha, N., Somashekhar, S.H., Sadashivappa, K. and Arun, K.V., 2012. Machining of soda lime glass using abrasive Hot Air Jet: An experimental Study. *Machining science and technology*, 16(3), pp.459-472.
- [25] Candiotti L.V., De Zan, M.M., Cámara M.S., and Goicoechea H.C., Experimental design and multiple response optimization. Using the desirability function in analytical methods development, *Talanta*, 124, (2014) pp.123-138.